Published in final edited form as:

Nature. 2013 November 21; 503(7476): 410–413. doi:10.1038/nature12642.

The Nuclear Receptor Rev-erbα Controls Circadian Thermogenic Plasticity

Zachary Gerhart-Hines[1,2], **Dan Feng**[#1,2], **Matthew J. Emmett**[#1,2], **Logan J. Everett**[1,2], **Emanuele Loro**[4,5], **Erika R. Briggs**[1,2], **Anne Bugge**[1,2], **Catherine Hou**[6], **Christine Ferrara**[7], **Patrick Seale**[2,3], **Daniel A. Pryma**[6], **Tejvir S. Khurana**[4,5], and **Mitchell A. Lazar**[1,2]

[1]Division of Endocrinology, Diabetes, and Metabolism, Department of Medicine, Department of Genetics, Perelman School of Medicine at the University of Pennsylvania, Philadelphia, PA 19104, USA

[2]The Institute for Diabetes, Obesity, and Metabolism, Perelman School of Medicine at the University of Pennsylvania, Philadelphia, PA 19104, USA

[3]Department of Cell and Developmental Biology, Perelman School of Medicine at the University of Pennsylvania, Philadelphia, PA 19104, USA

[4]Department of Physiology, Perelman School of Medicine at the University of Pennsylvania, Philadelphia, PA 19104, USA

[5]Pennsylvania Muscle Institute, Perelman School of Medicine at the University of Pennsylvania, Philadelphia, PA 19104, USA

[6]Department of Radiology, Perelman School of Medicine at the University of Pennsylvania, Philadelphia, PA 19104, USA

[7]Department of Pediatrics, Children's Hospital of Philadelphia, Philadelphia, PA 19104, USA

[#] These authors contributed equally to this work.

Abstract

Circadian oscillation of body temperature is a basic, evolutionary-conserved feature of mammalian biology[1]. Additionally, homeostatic pathways allow organisms to protect their core temperatures in response to cold exposure[2]. However, the mechanism responsible for coordinating daily body temperature rhythm and adaptability to environmental challenges is unknown. Here we

Address correspondence and requests for materials to: Mitchell A. Lazar, M.D., Ph.D., Phone: (215) 898-0198; lazar@mail.med.upenn.edu.

Author Contributions D.F., M.J.E., L.J.E., E.R.B., A.B., and C.F. performed key experiments/data analysis and read the manuscript. P.S. provided advice and read the manuscript. E.L. and T.S.K. designed, performed, and analyzed EMG studies and read the manuscript. C.H. and D.A.P. designed, performed, and analyzed ^{18}FDG scans and read the manuscript. Z.G.H. performed many experiments and Z.G.H. and M.A.L. conceived the project, designed experiments, analyzed all results, and wrote the manuscript.

Author Information Reprints and permissions information is available at www.nature.com/reprints.

The authors have no competing financial conflict of interest.

Supplementary Information is linked to the online version of the paper at www.nature.com/nature.

Full Methods and associated references are available in the online version of the paper.

show that the nuclear receptor Rev-erbα, a powerful transcriptional repressor, links circadian and thermogenic networks through the regulation of brown adipose tissue (BAT) function. Mice exposed to cold fare dramatically better at 5 AM (Zeitgeber time 22) when Rev-erbα is barely expressed than at 5 PM (ZT10) when Rev-erbα is abundant. Deletion of *Rev-erbα* markedly improves cold tolerance at 5 PM, indicating that overcoming Rev-erbα-dependent repression is a fundamental feature of the thermogenic response to cold. Physiological induction of uncoupling protein 1 (UCP1) by cold temperatures is preceded by rapid down-regulation of *Rev-erbα* in BAT. Rev-erbα represses UCP1 in a brown adipose cell-autonomous manner and BAT UCP1 levels are high in *Rev-erbα*-null mice even at thermoneutrality. Genetic loss of *Rev-erbα* also abolishes normal rhythms of body temperature and BAT activity. Thus, Rev-erbα acts as a thermogenic focal point required for establishing and maintaining body temperature rhythm in a manner that is adaptable to environmental demands.

The molecular clock is an autoregulatory network of core transcriptional machinery orchestrating behavioral and metabolic programming in the context of a 24-hour light-dark cycle[1,3]. The importance of appropriate synchronization in organismal biology is underscored by the robust correlation between disruption of clock circuitry and development of disease states such as obesity, diabetes mellitus, and cancer[4-6]. Tissue-specific clocks are entrained by environmental stimuli, blood-borne hormonal cues, and direct neuronal input from the superchiasmatic nucleus (SCN) located in the hypothalamus to ensure coordinated systemic resonance[1,7].

One of the defining metrics of circadian patterning is body temperature[8], which is highest in animals while awake and lowest while asleep[1]. A major site of mammalian thermogenesis is brown adipose tissue (BAT), which is characterized by high glucose uptake, oxidative capacity, and mitochondrial uncoupling[2]. Despite a substantial body of literature examining various regulatory aspects of BAT function and body temperature, little is known about the mechanisms controlling circadian thermogenic rhythms and, more importantly, how this patterning influences adaptability to environmental challenges. The circadian transcriptional repressor Rev-erbα has been previously linked to the regulation of glucose and lipid metabolism in tissues such as skeletal muscle, white adipose, and liver[9-15] but its influence on BAT physiology remains unknown.

Here we investigated the function of Rev-erbα in controlling temperature rhythms and thermogenic plasticity through integration of circadian and environmental signals. All experiments were performed on C57Bl/6 mice and, unless otherwise noted, at murine thermoneutrality (~29-30°C) to avoid confounding background contributions from the “browning” of white adipose depots or partial stimulation of BAT activity[16]. At thermoneutrality, the circadian oscillations of *Rev-erbα* gene expression (Fig. 1a) and protein levels (Supplementary Fig. 1a) in BAT were similar to other tissues[11,17], peaking in the light and being nearly absent in the dark. *Rev-erbα* ablation altered *Bmal1* transcription but did not affect the rhythmicity of *Rev-erbβ*, *Cry1-2*, *Per1-3*, nor *Clock* (Supplementary Fig. 1b), consistent with the mild circadian phenotype previously observed[17].

To evaluate the role of Rev-erbα in BAT, C57Bl/6 wild type (WT) and *Rev-erbα* KO mice were subjected to an acute cold challenge from ZT4-10 (11 AM - 5 PM) when Rev-erbα

levels peak in WT animals. In accordance with previous reports that thermoneutrally-acclimated C57Bl/6 mice fail to thrive during acute cold stresses[16,18,19], body temperatures of WT animals dropped markedly when shifted from 29°C to 4°C (Fig. 1b), and this inability to maintain body temperature was associated with failure to survive the cold exposure (Fig. 1c). By contrast, *Rev-erbα* KO mice maintained body temperature and uniformly survived the ZT4-10 cold challenge.

Notably, these studies were all performed during the day, when Rev-erbα peaks in WT mice. Since Rev-erbα is physiologically nearly absent at night, we next explored whether the circadian expression of *Rev-erbα* imposed a diurnal variation in cold tolerance. Previous studies of animals exposed to cold at either mid-morning or early afternoon reported modest differences in tolerance but this effect was believed to be a result of altered vasodilation[20]. Remarkably, during the dark period, when Rev-erbα levels are at the nadir of their physiological rhythm, WT mice were fully able to protect their body temperature and were phenotypically indistinguishable from *Rev-erbα* KO mice in both body temperature regulation (Fig. 1d) and survival (Fig. 1e) following cold challenge. These findings implicate Rev-erbα in establishing a circadian rhythm of cold tolerance through suppression of heat-producing pathways.

The increased cold tolerance of *Rev-erbα* KO mice was associated with higher oxygen consumption rates compared to WT littermates (Fig. 1f). Food intake (Supplementary Fig. 2a), basal muscle activity, and cold-induced shivering (Fig. 1g, Supplementary Fig. 2b) were unchanged between genotypes indicating that the Rev-erbα-dependent differences in oxidative capacity were likely due to alterations in BAT-driven, nonshivering thermogenic program. Indeed, brown adipose isolated from cold-challenged *Rev-erbα* KO animals consumed more oxygen than BAT from WT mice (Fig. 1h). Moreover, NE administration induced a larger increase in oxygen consumption in *Rev-erbα* KO animals than in control littermates (Supplementary Fig. 2c) with no genotypic difference in muscle activity (Supplementary Fig. 2d-e) further suggesting that Rev-erbα modulates heat production and cold susceptibility through BAT thermogenic pathways. Despite enhanced BAT metabolic capacity, *Rev-erbα* KO mice exhibited no significant difference in weight or food intake at room temperature and thermoneutrality compared to WT controls (data not shown) likely due to counteracting effects of Rev-erbα deletion in other tissues such as increased hepatic lipogenesis[9] or decreased skeletal muscle oxidative capacity[10].

Given the considerable influence that environmental demands have on BAT-mediated thermogenesis, we investigated whether Rev-erbα was subject to control by temperature in BAT. *Rev-erbα* levels normally rise between ZT4 and 10 (11 AM and 5 PM) in a circadian manner but cold exposure rapidly attenuated *Rev-erbα* expression (Fig. 2a) whereas closely-related nuclear receptor *Rev-erbβ* did not undergo a similar cold-dependent decrease (Supplementary Fig. 3a). Cold-mediated reduction of *Rev-erbα* gene expression occurred in parallel with the induction of *Bmal1*, an established target of Rev-erbα repression (Supplementary Fig. 3b), as well as the canonical thermogenic regulators uncoupling protein 1 (*Ucp1*) (Fig. 2a) and peroxisome proliferator-activated receptor gamma coactivator 1 alpha (*Pgc-1α*)[21] (Supplementary Fig. 3c). *Rev-erbα* expression was attenuated following both moderate (29°C to 20°C) and acute (29°C to 4°C) cold stresses (Supplementary Fig.

3d). Similarly, Rev-erbα protein plummeted when mice were shifted to 4°C (Fig. 2b). Classically, regulation of brown adipose thermogenesis has been attributed predominantly to sympathetic release of NE and subsequent activation of adrenergic signaling cascades[2]. We therefore considered whether the cold-induced decrease in Rev-erbα levels was related to the adrenergic pathway. However, whereas the highly cAMP-sensitive nuclear receptor NOR1[22] was induced comparably by NE and cold (Fig. 2c), NE administration did not mimic the effect of cold exposure on expression of *Rev-erbα* gene (Fig. 2c) or protein (Supplementary Fig. 3e). This is consistent with reports that pan-sympathomimetic stimulation does not fully recapitulate cold-mediated BAT activation in humans[23,24], and suggests that the role of Rev-erbα in thermogenic regulation is independent of sympathetic stimulation.

The rapidity with which Rev-erbα was reduced in the cold and its inverse relationship to *Ucp1* expression suggested that Rev-erbα might elicit thermogenic regulation through active repression of the *Ucp1* gene. Indeed, at thermoneutrality *Ucp1* mRNA (Fig. 3a) and protein levels (Fig. 3b) were elevated in the BAT of *Rev-erbα* KO mice, consistent with the more pronounced metabolic response of these mice to cold exposure or NE administration. BAT *Ucp1* in *Rev-erbα* KO mice was only modestly further increased upon cold challenge compared to WT animals (Fig. 3a-b), suggesting that Rev-erbα down-regulation is an integral component of the physiological *Ucp1* induction following cold exposure. Consistent with recent work on the temporal correlation between *Ucp1* mRNA and protein levels, we did not observe significant cold-mediated changes in UCP1 protein in the acute time frame in which we performed our cold challenges[25]. Increases in *Ucp1* were not seen in white adipose depots or skeletal muscle (data not shown), signifying a BAT-specific phenomenon. *Bmal1* mRNA and protein followed a similar pattern to *Ucp1* (Supplementary Fig. 4a-b) whereas *Pgc-1α* levels were unchanged between control and *Rev-erbα* KO animals at thermoneutrality, and were comparably cold-induced, suggesting *Rev-erbα*-independence (Supplementary Fig. 4a-b). Nevertheless, Rev-erbα controlled expression of *Ucp1*, which is critical for nonshivering heat production in BAT[2,19]. Underscoring this point, *Ucp1* mRNA levels were basally higher in *Rev-erbα* KO mice given only saline than those of NE-treated WT animals and were not increased further when NE was administered to the *Rev-erbα* KOs (Fig. 3c).

Ucp1 was elevated in primary brown adipocytes lacking *Rev-erbα* and ectopic expression of *Rev-erbα* restored *Ucp1* mRNA to WT levels, whereas overexpression of *Rev-erbα* in WT adipocytes caused no further effect (Fig. 3d) illustrating that Rev-erbα represses *Ucp1* in a BAT cell-autonomous manner. Consistent with these findings, Rev-erbα binding was detected at the *Ucp1* gene locus, and this binding decreased after cold challenge (Fig. 3e). *Ucp1* displayed a rhythmic expression profile anti-phase to *Rev-erbα* in primary brown adipocytes cultured *ex vivo* and synchronized by serum shock (Supplementary Fig. 4c). This *Ucp1* circadian rhythmicity was completely abolished in *Rev-erbα* KO animals (Fig. 3f). These data establish Rev-erbα as a direct, negative regulator of thermogenic transcriptional programs.

The ability of Rev-erbα to repress BAT heat production and impose a circadian pattern of cold tolerance prompted us to investigate whether Rev-erbα influenced body temperature

rhythm. *Rev-erbα* ablation dramatically altered body temperature oscillation, both of the core (Fig. 4a) and interscapular region (BAT) (Fig. 4b). Higher body temperature was maintained by *Rev-erbα* KO animals throughout the light phase, indicating that Rev-erbα was required for daily depressions in thermogenic rhythmicity**.** Indeed, thermographic surface measurements showed that *Rev-erbα* KO mice were warmer than WT mice from ZT4-10 (11 AM - 5 PM) but not ZT16-22 (11 PM - 5 AM) (Fig. 4c, Supplementary Fig. 5a). Comparison between colonic and interscapular temperatures implicated BAT as the primary source of the genotypic variation (Supplementary Fig. 5b). We note that previous studies of thermoregulation in mice lacking *Rev-erbα* were performed at room temperature, which could confound the assessment of Rev-erbα's role in BAT thermogenesis[13,16].

To address the effect of Rev-erbα on the circadian control of BAT function, we measured glucose uptake using 18-fluorodeoxyglucose positron emission tomography (^{18}FDG-PET)[26-28]. Strikingly, the diurnal oscillation of BAT glucose uptake[29] was abolished by deletion of *Rev-erbα* (Fig. 4d, Supplementary Fig. 5c). Glucose uptake was higher in *Rev-erbα* KO mice than control littermates during the day and did not increase at night as in WT animals (Fig. 4e). These results indicate that Rev-erbα is required for the circadian rhythm of body temperature and BAT activity (Supplementary Fig. 6).

Daily oscillation in body temperature is one of the most basic and defining characteristics of mammalian circadian biology[6]. The present findings suggest a mechanism whereby circadian and cold-regulated networks converge on Rev-erbα in BAT to establish and maintain thermogenic rhythmicity while affording the organism an adaptability to rapidly respond to external temperature stresses. Rev-erbα acts as a focal point, integrating the continuity of circadian rhythms with the variability of environmental challenges. Rev-erbα alone is sufficient to modulate brown adipose function, which is in contrast to the redundancy found between both nuclear receptors Rev-erbα and Rev-erbβ in controlling hepatic physiology[11,12]. The fact that *Rev-erbβ* is not subject to similar cold-dependent regulation ensures that temperature stresses can target appropriate programs without detriment to the BAT core clock machinery.

The function of BAT as a professional heat-producing tissue likely evolved to permit eutherian mammals to survive exposure to an array of environmental demands[30]. However, from an evolutionary standpoint, constitutive, UCP1-mediated dissipation of the mitochondrial proton gradient would be wasteful and unfavorable when resources are scarce and increased heat production is unnecessary. Our data are consistent with a model of Rev-erbα-controlled BAT thermogenesis that provides an energetic checks- and-balances system. Circadian rhythm of Rev-erbα imposes an oscillation in brown adipose activity, increasing body temperature when mammals are awake and potentially exposed to harsh environmental conditions and depressing thermogenesis during sleep when mammals are typically in protective shelter and require little facultative heat production. In the event that the animal is confronted by a sudden temperature challenge while sleeping, rapid reduction in Rev-erbα would facilitate appropriate induction of thermogenic programs and organismal survival.

Methods

Animal Studies

All animal studies were performed with an approved protocol from the University of Pennsylvania Perelman School of Medicine Institutional Animal Care and Use Committee. The *Rev-erbα* KO mice were obtained from B. Vennström and backcrossed seven or more generations with C57Bl/6 mice. Mice were housed on a 12:12-h light-dark cycle (lights on at 7 AM, lights off at 7 PM). Gene expression, protein analysis, and temperature measurements were carried out on 12-16 week old male *Rev-erbα* KO mice and WT littermates. Cold exposure experiments were performed in climate-controlled rodent incubators set to 29°C and 4°C. All WT and *Rev-erbα* KO mice used in the studies were first placed in individual cages with access to food and water and allowed to acclimate to 29°C for 2 weeks prior to cold challenge. For NE administration experiments, thermoneutrally-acclimated WT and *Rev-erbα* KO mice were given 1 mg/kg L-(-)-NE-bitartrate salt monohydrate (Sigma). Mice were injected subcutaneously for NE-induced oxygen consumption assays but intraperitoneally for all other procedures.

Whole Animal Oxygen Consumption Rate

Oxygen consumption rates were measured using comprehensive lab animal monitoring system (CLAMS) metabolic cages contained with temperature-controlled rodent incubators. Cold-induced oxygen consumption rates were assessed on singly-housed, unanaesthetized WT and *Rev-erbα* KO mice. Temperature of the housing unit was transitioned from 29°C to 4°C over the course of 20-30 min and mice were then cold challenged for an additional 2 h. NE-induced oxygen consumption rates were assessed as previously described[16]. Briefly, mice were anaesthetized with 75 mg/kg pentobarbital intraperitoneally and placed in a CLAMS unit set to 33°C to maintain body temperature. One mg/kg NE was administered subcutaneously once a baseline oxygen consumption rate had been obtained (approximately 20 min after pentobarbital injection). NE-induced oxygen consumption was then measured until rates had peaked and started declining (approximately 90 min after NE administration).

Temperature Measurements

Core and brown adipose temperature measurements were obtained using surgically implanted dataloggers for core (SubCue Dataloggers) and telemetric transmitters for BAT (IPTT 300 transponders, Biomedic data systems) following pentobarbital anesthetization. Mice were maintained at 29°C and monitored daily and surgical sites were treated with bacitracin to prevent discomfort. Following a week of convalescence, temperature measurements were recorded. Colonic and interscapular surface measurements were obtained using YSI Precision Thermometers with rectal or banjo probe attachments, respectively.

Immunoblotting

BAT samples were homogenized in RIPA (137 mM NaCl, 0.1% SDS, 0.5% Na-deoxycholate, 1% NP-40, 20 mM NAF, and 20 mM G2P in 1X PBS pH 7.4, supplemented with Complete protease inhibitors (Roche)) using a Tissuelyser (Qiagen) for 1.5 min at a

frequency of 20 s^{-1} followed by sonication using a Bioruptor (Diagenode) for 30 sec on the "high" setting. SDS-PAGE was performed using 50 mg of protein loaded onto a 10% Tris-glycine gel (Invitrogen), followed by transfer to a PVDF membrane (Invitrogen). After antibody incubation, blots were developed using the SuperSignal West Dura chemiluminescence kit from Pierce.

Cell Culture

Preadipocytes were harvested from BAT depots of pups that were between postnatal days 1-3. Depots were minced finely using spring scissors (Roboz) in DMEM/F-12 GlutaMax (Invitrogen) before addition of 1.5 U/ml Collagenase D (Roche) and 2.4 U/ml Dispase II (Roche) and incubation in a 37°C shaking water bath for 45 minutes. Cells were purified through 100 μm filters (Millipore), pelleted and resuspended in Growth media [DMEM/F-12 GlutaMax supplemented with 10% Fetal Bovine Serum (Tissue Culture Biologicals), HEPES pH 7.2 (Invitrogen), and Penicillin/Streptomycin (Invitrogen)]. Adipocyte differentiation was induced upon confluence with Induction media (Growth media supplemented with 500 nM Dexamethasone, 125 nM Indomethacin, 0.5 mM IBMX, 1 nM Rosiglitazone, 1 nM T3, and 20 nM Insulin) for 36 h. Following induction, cells were cultured in Maintenance media (Growth media supplemented with 1 nM T3 and 20 nM Insulin). Serum synchronization was performed by incubating differentiated adipocytes with DMEM/F-12 GlutaMax containing 50% Horse Serum for 2 h. Following two washes in PBS, cells were placed in DMEM/F-12 GlutaMax containing 0.5% Fetal Bovine Serum, 1 nM T3, and 20 nM Insulin and total RNA was harvested at the indicated time points. For ectopic *Rev-erbα* expression, primary adipocytes were electroporated 36 h after removing Induction media using an Amaxa Cell Line Nucleofector Kit L (Lonza) according to manufacturer's instructions and harvested 48 h later.

Thermographic Imaging

Thermography was performed by the Penn Mouse Phenotyping, Physiology, and Metabolism (MPPM) core during the light and dark phases using a FLIR SC620 infrared camera on WT and *Rev-erbα* KO mice acclimated at thermoneutrality for 2 weeks. No anesthesia was used in order to avoid confounding effects on body temperature.

Fluorodeoxyglucose Imaging

^{18}Fluorodeoxyglucose (^{18}FDG) imaging was performed in the University of Pennsylvania Small Animal Imaging Facility (SAIF). Doses of saline containing 300 μCi ^{18}FDG were administered through the lateral tail vein under constant isoflurane anesthesia (1-2%, 1 L O_2/min). Mice were scanned on a Philips Mosaic HP 1 h after injection. Percent injected dose was calculated by assessing the ratio of radioactive counts in the region of interest (ROI) for brown adipose to the total counts for the animal using Amide medical imaging software.

BAT Oxygen Consumption Rate

Mice were housed at thermoneutrality for one week and subjected to a 1 h cold challenge (4°C) starting at 1 PM. The interscapular BAT depot of each mouse was harvested and

divided into eleven pieces, weighing between 1.5 and 2 mg, and washed 3 times in Seahorse XF assay media supplemented with 25 mM glucose and 1 mM sodium pyruvate and adjusted to pH 7.4. Subsequently, the BAT pieces were placed individually in the center of a well of a Seahorse XF24 islet capture microplate and held in place by overlaying a capture screen followed by addition of 675 μl of the supplemented Seahorse XF assay media. The oxygen consumption rate of each well was measured 3 times for 2 min following 3 min of mixing and a 2 min wait on the Seahorse XF24 analyzer (Seahorse Bioscience). The results from the 11 wells of each genotype was averaged and normalized to total mg of tissue.

Electromyogram (EMG)

EMG recordings were made essentially as previously described[19]. Three 29 gauge needle electrodes (2 recording electrodes 4 mm apart and 3 mm deep and 1 reference electrode placed distally) were fixed transcutaneously for acquiring the EMG signal from the scapular muscles. For optimal stability, recording electrodes were placed into 4 mm diameter plastic tubes (1 mL serological pipettes), and juxtaposed using polyolefin tubing. The entire electrode set was introduced into the scapular region of prone mice using a micromanipulator (WPI). The EMG signal was processed (low-pass filter 3 kHz, high-pass filter 10 Hz, notch filter 60 Hz) and amplified 1000X with a P55 differential amplifier (Grass Instruments, Quincy, MA). Data were A/D converted and recorded with a PowerLab 8SP at a sampling frequency of 10 kHz (ADInstruments, Colorado Springs, CO). The signal was acquired and Root Mean Square (RMS) of the EMG signal was calculated with LabChart 7 (ADInstruments).

For cold induced shivering, mice were exposed to 4°C for 1 h, quickly anesthetized with isoflurane and placed on a temperature controlled pad maintained at 15°C. EMG signals were recorded for 15 min and the data collected between minutes 2 and 7 were used for the analyses. Mice were allowed to recover for one day and then subjected to EMG measurement at thermoneutrality, maintaining the temperature controlled pad at 33°C.

For recording norepinephrine (NE)-induced EMGs, mice were anesthetized with an IP injection of 75 mg/kg pentobarbital. The temperature controlled pad was maintained at 33°C. After obtaining 5 min of basal EMG recordings, 1 mg/kg NE was injected subcutaneously on the back of the mouse and the recording continued for 20 min. All RMS calculations were made from 2 min of data collected prior to NE administration as well as 5, 10 and 15 min after NE administration.

ChIP

Murine BAT was harvested immediately after euthanasia. It was quickly minced and cross-linked in 1% formaldehyde for 20 min, followed by quenching with 1/20 volume of 2.5 M glycine solution and two washes with ice-cold PBS. Chromatin fragmentation was performed by sonication in ChIP SDS lysis buffer (50 mM HEPES, 1% SDS, 10 mM EDTA at pH 7.5) using probe sonication. Proteins were immunoprecipitated in ChIP dilution buffer (50 mM HEPES, 155 mM NaCl, 1.1% Triton X-100, 0.11% Na-deoxycholate, Complete protease inhibitor tablet at pH 7.5). Cross-linking was reversed overnight at 65°C in elution buffer (50 mM Tris-HCL, 10 mM EDTA, 1% SDS at pH 8), and DNA was isolated using

phenol/chloroform/isoamyl alcohol. Precipitated DNA was analyzed by quantitative PCR. ChIP experiments were performed independently on BAT samples from three mice harvested at 5 PM with or without a 6 h cold challenge as previously described[11]. ChIP of Rev-erbα was performed using the Cell Signaling Technology antibody (#2124). Deep sequencing was carried out by the Functional Genomics Core (J. Schug and K. Kaestner) of the Penn Institute for Diabetes, Obesity, and Metabolism using the Illumina Genome Analyzer IIx and Illumina HiSeq 2000 and sequences were obtained using the Solexa Analysis Pipeline.

RNA

Total RNA was isolated from BAT tissue by Trizol (Invitrogen) extraction and 1.5 μg of total RNA was used for cDNA synthesis using the High-Capacity cDNA Reverse Transcription kit (Applied Biosystems). Relative mRNA levels were determined using quantitative PCR and normalization to housekeeping gene 36B4. Primer sequences are available upon request.

Statistics

Data are presented as means ± s.d. unless otherwise noted. Statistical analysis was performed using Student's t-test for comparisons between two groups, one-way analysis of variance (ANOVA) with multiple comparisons for assessment of more than two groups on GraphPad Prism software. Comparisons among specific groups were done using post-tests as indicated in the respective figure legends.

Supplementary Material

Refer to Web version on PubMed Central for supplementary material.

Acknowledgements

We thank the Functional Genomics Core (J. Schug) and the Mouse Phenotyping, Physiology, and Metabolism Core (R. Ahima and R. Dhir) of the Penn Diabetes Research Center (NIH P30 DK19525). We also thank the Small Animal Imaging Facility of the Perelman School of Medicine at the University of Pennsylvania (E. Blankemeyer). This work was supported by NIH grants R01 DK45586 (M.A.L.) and F-32 DK095563 (Z.G.H.), and the JPB Foundation. A.B. was funded by the Novo Nordisk STAR postdoctoral program.

References

1. Bass J. Circadian topology of metabolism. Nature. 2012; 491:348–356. [PubMed: 23151577]
2. Cannon B, Nedergaard J. Brown adipose tissue: function and physiological significance. Physiol. Rev. 2004; 84:277–359. [PubMed: 14715917]
3. Takahashi JS, Hong H-K, Ko CH, McDearmon EL. The genetics of mammalian circadian order and disorder: implications for physiology and disease. Nat. Rev. Genet. 2008; 9:764–775. [PubMed: 18802415]
4. Sahar S, Sassone-Corsi P. Metabolism and cancer: the circadian clock connection. Nat. Rev. Cancer. 2009; 9:886–896. [PubMed: 19935677]
5. Asher G, Schibler U. Crosstalk between components of circadian and metabolic cycles in mammals. Cell Metab. 2011; 13:125–137. [PubMed: 21284980]
6. Bass J, Takahashi JS. Circadian integration of metabolism and energetics. Science. 2010; 330:1349–1354. [PubMed: 21127246]

7. Feng D, Lazar MA. Clocks, metabolism, and the epigenome. Mol. Cell. 2012; 47:158–167. [PubMed: 22841001]
8. Buhr ED, Yoo S-H, Takahashi JS. Temperature as a universal resetting cue for mammalian circadian oscillators. Science. 2010; 330:379–385. [PubMed: 20947768]
9. Feng D, et al. A circadian rhythm orchestrated by histone deacetylase 3 controls hepatic lipid metabolism. Science. 2011; 331:1315–1319. [PubMed: 21393543]
10. Woldt E, et al. Rev-erb-α modulates skeletal muscle oxidative capacity by regulating mitochondrial biogenesis and autophagy. Nat. Med. 2013 doi:10.1038/nm.3213.
11. Bugge A, et al. Rev-erbα and Rev-erbβ coordinately protect the circadian clock and normal metabolic function. Genes Dev. 2012; 26:657–667. [PubMed: 22474260]
12. Cho H, et al. Regulation of circadian behaviour and metabolism by Rev-erb-α and Rev-erb-β. Nature. 2012; 485:123–127. [PubMed: 22460952]
13. Delezie J, et al. The nuclear receptor Rev-erbα is required for the daily balance of carbohydrate and lipid metabolism. FASEB J. 2012; 26:3321–3335. [PubMed: 22562834]
14. Le Martelot G, et al. Rev-erbalpha participates in circadian SREBP signaling and bile acid homeostasis. PLoS Biol. 2009; 7:e1000181. [PubMed: 19721697]
15. Solt LA, et al. Regulation of circadian behaviour and metabolism by synthetic Rev-erb agonists. Nature. 2012; 485:62–68. [PubMed: 22460951]
16. Cannon B, Nedergaard J. Nonshivering thermogenesis and its adequate measurement in metabolic studies. J. Exp. Biol. 2011; 214:242–253. [PubMed: 21177944]
17. Preitner N, et al. The orphan nuclear receptor Rev-erbalpha controls circadian transcription within the positive limb of the mammalian circadian oscillator. Cell. 2002; 110:251–260. [PubMed: 12150932]
18. Lim S, et al. Cold-induced activation of brown adipose tissue and adipose angiogenesis in mice. Nat Protoc. 2012; 7:606–615. [PubMed: 22383039]
19. Golozoubova V, et al. Only UCP1 can mediate adaptive nonshivering thermogenesis in the cold. FASEB J. 2001; 15:2048–2050. [PubMed: 11511509]
20. Talan MI, Tatelman HM, Engel BT. Cold tolerance and metabolic heat production in male C57BL/6J mice at different times of day. Physiol. Behav. 1991; 50:613–616. [PubMed: 1801018]
21. Puigserver P, et al. A cold-inducible coactivator of nuclear receptors linked to adaptive thermogenesis. Cell. 1998; 92:829–839. [PubMed: 9529258]
22. Pearen MA, et al. The orphan nuclear receptor, NOR-1, is a target of beta-adrenergic signaling in skeletal muscle. Endocrinology. 2006; 147:5217–5227. [PubMed: 16901967]
23. Cypess AM, et al. Cold but not sympathomimetics activates human brown adipose tissue in vivo. Proc. Natl. Acad. Sci. U.S.A. 2012; 109:10001–10005. [PubMed: 22665804]
24. Vosselman MJ, et al. Systemic β-adrenergic stimulation of thermogenesis is not accompanied by brown adipose tissue activity in humans. Diabetes. 2012; 61:3106–3113. [PubMed: 22872233]
25. Nedergaard J, Cannon B. UCP1 mRNA does not produce heat. Biochim. Biophys. Acta. 2013 doi: 10.1016/j.bbalip.2013.01.009.
26. Cypess AM, et al. Identification and importance of brown adipose tissue in adult humans. N. Engl. J. Med. 2009; 360:1509–1517. [PubMed: 19357406]
27. Van Marken Lichtenbelt WD, et al. Cold-activated brown adipose tissue in healthy men. N. Engl. J. Med. 2009; 360:1500–1508. [PubMed: 19357405]
28. Virtanen KA, et al. Functional brown adipose tissue in healthy adults. N. Engl. J. Med. 2009; 360:1518–1525. [PubMed: 19357407]
29. Van der Veen DR, Shao J, Chapman S, Leevy WM, Duffield GE. A diurnal rhythm in glucose uptake in brown adipose tissue revealed by in vivo PET-FDG imaging. Obesity (Silver Spring). 2012; 20:1527–1529. [PubMed: 22447290]
30. Saito S, Saito CT, Shingai R. Adaptive evolution of the uncoupling protein 1 gene contributed to the acquisition of novel nonshivering thermogenesis in ancestral eutherian mammals. Gene. 2008; 408:37–44. [PubMed: 18023297]

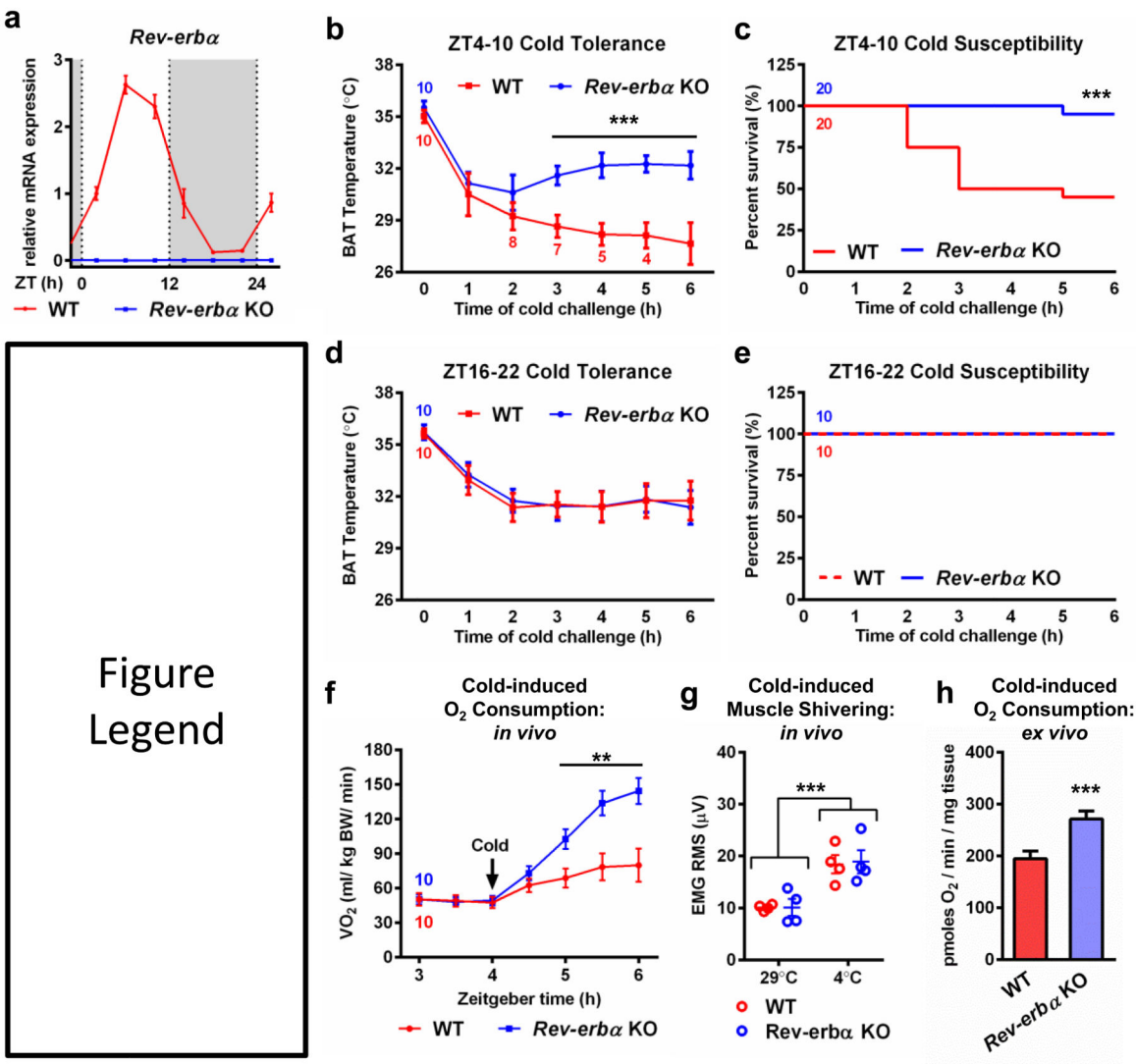

Figure 1. Rev-erbα mediates the circadian patterning of cold tolerance

a, *Rev-erbα* mRNA (n=3) in BAT of WT and *Rev-erbα* KO mice. **b**, Cold tolerance tests (CTT) and, **c**, survival curves for *Rev-erbα* KO mice and control littermates from ZT4-10 (11 AM-5 PM). **d**, CTTs and, **e** survival curves from ZT16-22 (11 PM-5 AM). The numbers of *Rev-erbα* KO and control mice in the CTT are indicated above or below the first data point, respectively; subsequent designations at data points are made if any animals were removed for having a temperature below 25°C. **f**, Oxygen consumption rate (n=10) and, **g**, electromyogram (EMG) (n=4) measurements of cold-challenged *Rev-erbα* KO mice and WT controls. **h**, Oxygen consumption rates of BAT isolated from animals exposed to cold for 1 h (n=3). ** p <0.01, *** p <0.001 as analyzed by two-tailed Student's t-test, one-way ANOVA, or Gehan-Breslow-Wilcoxon and Log-rank (Mantel-Cox) tests for the survival curves. Data are expressed as mean ± s.d.

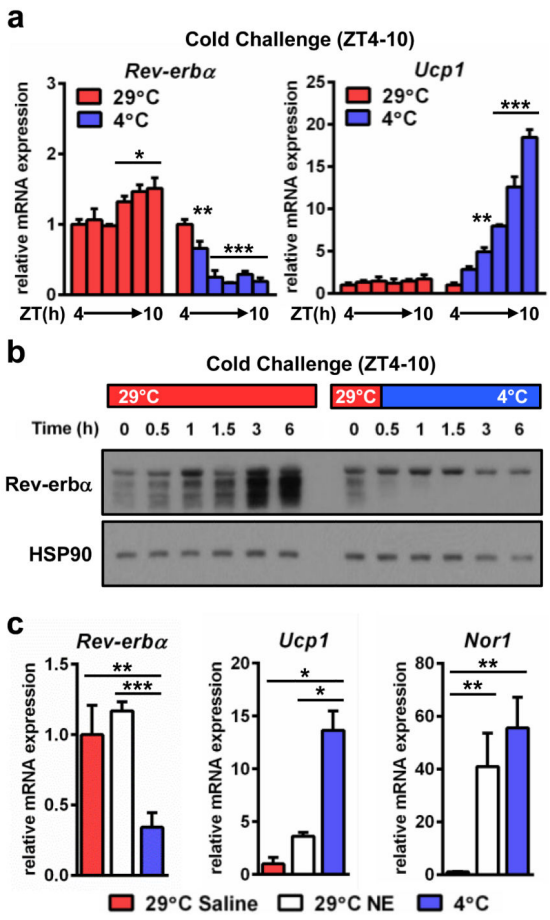

Figure 2. Cold stress rapidly down-regulates Rev-erbα

a, BAT mRNA (n=3) and, **b**, protein levels from WT mice following a cold exposure time course (n=2; each lane of the western blot represents pooled biological duplicates). **c**, BAT mRNA (n=3) following 3 h NE administration (1 mg/kg i.p.) or cold exposure (n=3). * $p<0.05$, ** $p<0.01$, *** $p<0.001$ as determined by one-way ANOVA with multiple comparisons and a Tukey post-test. Data are expressed as mean ± s.d.

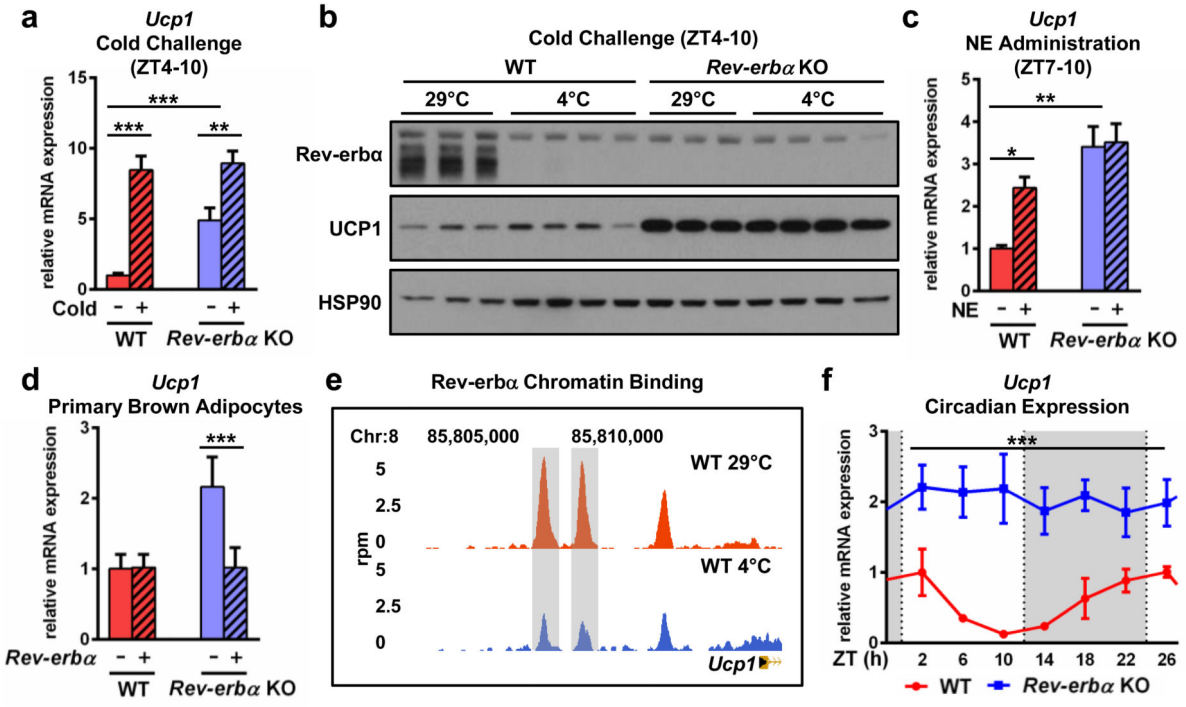

Figure 3. Rev-erbα represses thermogenic programming

a, BAT mRNA (n=6) and, **b**, protein from WT and *Rev-erbα* KO mice acutely exposed to cold for 6 h from ZT4-10. **c**, BAT mRNA following 3 h of NE administration from ZT7-10 (1 mg/kg i.p.) (n=3). **d**, *Ucp1* mRNA levels in preadipocytes isolated from *Rev-erbα* KO mice and WT littermates in which either *Rev-erbα* or vector control has been ectopically expressed (n=4). **e**, Rev-erbα occupancy at the *Ucp1* proximal promoter. Rev-erbα-specific peaks are shaded. **g**, *Ucp1* gene expression in BAT over a 24 h period (n=3). * p<0.05, ** p<0.01, *** p <0.001 as determined by two-tailed Student's t-test or one-way ANOVA with multiple comparisons and a Tukey post-test. Data are expressed as mean ± s.d.

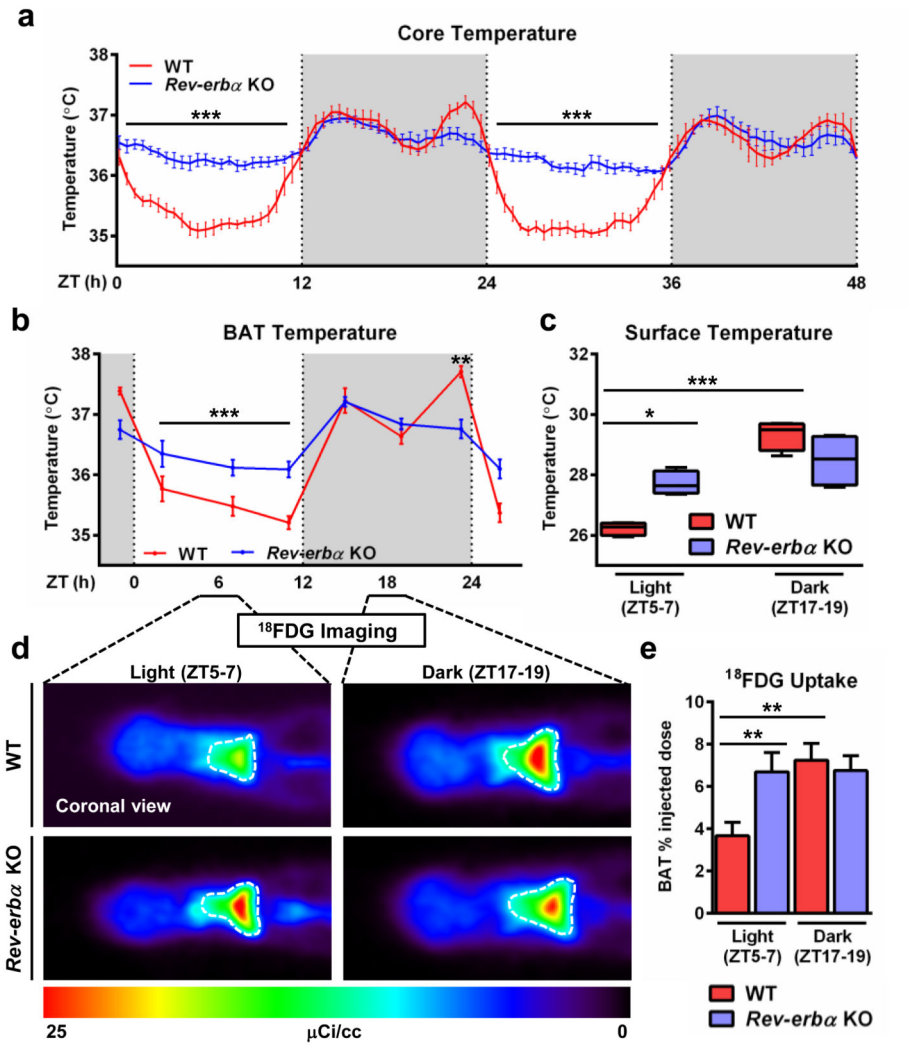

Figure 4. Rev-erbα orchestrates daily rhythms of body temperature and BAT activity

a, Core (n=6) and, **b**, BAT (n=10) temperatures measured from subcutaneously implanted thermometers. **c**, Quantified thermographic measurements of surface temperature (n=5) and, **d**, 18-fluorodeoxyglucose (^{18}FDG) imaging (n=4) of *Rev-erbα* KO mice and WT littermates during the light and dark phases. Representative coronal planes are shown for each group. **e**, Percent injected dose of ^{18}FDG in the BAT of animals from the study in 4d. * $p<0.05$, ** $p<0.01$, *** $p<0.001$ as determined by two-tailed Student's t-test or one-way ANOVA with multiple comparisons and a Tukey post-test. Data in 4a are expressed as rolling averages (±2 time points) ± s.e.m.; data in 4b are expressed as mean ± s.e.m.; data in 4c are expressed as a max to min box-and-whiskers plot; data in 4e are expressed as a mean ± s.d.